Linear Robust Adaptive Output-feedback Control of Chaotic PM Motors

Antonio Loria

Linear Robust Adaptive Output-feedback Control of
Chaotic PM Motors

Antonio Loría

Abstract— We solve the problems of set-point and tracking control of permanent-magnet synchronous motors with unknown load via *linear* angular-velocity-feedback control. We firstly assume that the motor parameters are known (except for the torque load) and show global exponential stability of the closed-loop system with a linear controller that uses only angular velocity measurements. Input to state stability follows as a corollary. We show how the latter may be enhanced via an additional current feedback. The controllers are also robust with respect to measurement noise and parametric uncertainty.

I. INTRODUCTION

One of the key problems related to the permanent-magnet synchronous motors (PMSM) is its natural *chaotic* behavior, for certain choices of parameters and initial conditions, see for instance [1], [2], [3], [4]. Then, it is desirable to control the chaotic PMSM to different regimes: set-point *i.e.*, constant angular velocity, and time-varying reference tracking control. Moreover, as is often desirable in control theory and practice, the control goal is to be achieved for all initial conditions that is, one seeks for *global* results. Of particular interest (at least in electrical engineering and physics) is to drive the PMSM to a constant operating point from initial conditions leading to chaos in open-loop –*cf.* [5], [6], [7]. The latter two exploit the Hamiltonian structure of the system, the design in [6] leads to a closed-loop system with multiple equilibria and the result is shown to hold for *almost* all initial conditions. While no stability proof is provided in [5] the control is interesting in that it also exploits the dissipative forces inherent in the system and yields good performance, in *simulations*. Adaptive set-point control algorithms are included in [6] (known parameters, unknown load) and in [8] (zero load, one unknown parameter, smooth-air gap machine). Other works aiming at annihilating chaos include [1] where the goal is to drive the machine to describe periodic orbits.

While a number of works concentrate on the task of eliminating (undesirable) chaotic behaviors, others focus on the opposite task with certain interesting applications in mind: [9] presents a controller to generate chaotic behavior in PMSMs used to construct vibratory soil compactors. In [10] chaos is induced via delayed feedback and some simulation results are presented.

In this paper we propose very simple output-feedback controllers and show that uniform exponential stability may be achieved even in the case that the torque load is unknown. By "output-feedback" it is meant that only shaft angular velocity measurements are used. As a direct corollary of the main results

The authors are with with C.N.R.S. at Laboratoire des Signaux et Systèmes, Supélec, 3, Rue Joliot Curie, 91192 Gif s/Yvette, France. E-mail: `loria@lss.supelec.fr`.

several natural robustness improvements may be obtained. In particular, Input-to-State Stability of the closed-loop system readily follows and it may be enforced by additional (current feedback). In simulations, we show that the controllers are also robust to parametric (time-varying) uncertainty and measurement noise.

The rest of the paper is organized as follows. In the forecoming section we present the dynamic model; in Section III we present our main results; the latter are illustrated in simulations in Section V and we conclude with some remarks in Section VI.

II. THE MODEL

A. *The physical model*

We adopt the "unified theory" of [11] which includes certain simplifications to obtain a tractable model; in particular, saturation of the iron core and the effects of the iron yokes are neglected. Therefore, it is assumed that inductances are current-independent. Furthermore, following a standard transformation, the dynamic model of the PMSM may be expressed in the *d-q* axes coordinates *i.e.*,

$$\frac{di_d}{dt'} = \frac{1}{L_d}\left[v_d - Ri_d + \omega L_q i_q\right] \tag{1a}$$

$$\frac{di_q}{dt'} = \frac{1}{L_q}\left[v_q - Ri_q - \omega L_d i_d - \omega \psi_r\right] \tag{1b}$$

$$\frac{d\omega}{dt'} = \frac{1}{J}\left[n_p \psi_r i_q + n_p(L_d - L_q)i_d i_q - \tau_L - \beta\omega\right] \tag{1c}$$

where t' denotes time. The variables carrying the index q are referred to the *quadrature*-axis and those carrying an index d are referred to the *direct* axis. As is customary the variables i represent currents, v represent input voltages (control inputs up to a gain); R corresponds to the stator resistance. After applying the transformation to the *d-q* coordinates axes, the inductances L_q, L_d become constant. The rest of the variables represent the permanent-magnet flux (ψ_r), the number of pole pairs n_p, the viscous friction coefficient (β), and the polar moment of inertia (J). The angular velocity is represented by ω and, finally, τ_L corresponds to the external-load torque. The latter two are of obvious practical interest from a control viewpoint.

The advantage of the model (1) is that inductances are constant (but not necessarily equal). More detailed models and descriptions of the PM dynamics can be found for instance in [2], [4], [12]. Simplified models are often used as well, for instance, neglecting viscous friction –*cf.* [6], [7] or by considering the stator inductances L_q, L_d to be equal, that is the case of the smooth-air gap PM machines –*cf.* [1], [3], [13], [9], [10], [14]. Our main results cover but are not limited to these cases. Other *d-q* models, such as that in [15] incorporate rotor-position back-emf

terms in the context of torque ripple minimization; see also [16] where the same model is used in the context of observer design for sensor-less control.

Alternatively, for models considering explicitly the nonlinear dependence of the inductances on the currents see for instance the series of fairly recent papers [17], [18], [19], [20] which deal with the *surface-mounted* PMSM and in a context well beyond the scope of this paper. See also [21] where the authors propose a model incorporating effects such as saturation of the iron core, cross-coupling, cross-saturation and slotting which yield current and position-dependent flux linkage equations. Flux variations are showed in experimentation.

To some extent, modelling errors entailed by neglecting saturation may be by considered as (time-varying) parameter uncertainty –*cf.* [11] and additive disturbances. Therefore, we show *analytically* that the controlled system under our approach is robust (ISS) with respect to external perturbations and, in simulations, we show that the controller is also robust with respect to time-varying parameter uncertainties and measurement noise. Other articles where parameter uncertainty, albeit *constant*, is considered include [5], [22], [23], [8]. The last three deal with adaptive control problems in particular, in [8] parameter convergence is showed under the assumption of smooth air-gap (constant equal inductances). In the article [5] a robustness approach is taken to show, in simulations, that the controlled machine remains practically asymptotically stable. In all of the latter the model (1) is used; except for [23] where it is further assumed that inductances are equal and constant (*i.e.,* $\varepsilon = 0$).

B. The control model

For control purposes, we recall a standard transformation of system (1) to put the dynamical model in an equivalent form more "comfortable" for control design purposes; this is used in most of the cited references. Let

$$T := \begin{bmatrix} bk & 0 & 0 \\ 0 & k & 0 \\ 0 & 0 & R/L_q \end{bmatrix}, \quad b := \frac{L_q}{L_d}, \quad k := \frac{\beta R}{L_q n_p \tau \psi_r}$$

$$\gamma := -\frac{\psi_r}{kL_q}, \quad \sigma := \frac{\beta L_q}{RJ}, \quad \varepsilon := \frac{n_p b L_q^2 k^2 (L_q - L_d)}{JR^2},$$

$$\hat{u}_d := \frac{v_d}{Rk}, \quad \hat{u}_q := \frac{v_q}{Rk}, \quad \tilde{\tau}_L := \frac{L_q^2 \tau_L}{JR^2}.$$

Then, the system (1) may be written in the dimension-less compact form

$$\frac{d\tilde{\imath}_d}{dt} = -\tilde{\imath}_d + \tilde{\omega}\tilde{\imath}_q + \hat{u}_d \quad (2a)$$

$$\frac{d\tilde{\imath}_q}{dt} = -\tilde{\imath}_q - \tilde{\omega}\tilde{\imath}_d + \gamma\tilde{\omega} + \hat{u}_q \quad (2b)$$

$$\frac{d\tilde{\omega}}{dt} = \sigma(\tilde{\imath}_q - \tilde{\omega}) + \varepsilon\tilde{\imath}_d\tilde{\imath}_q - \tilde{\tau}_L \quad (2c)$$

where time has been redefined to $t := Rt'/L_q$ and the state variables as $(\tilde{\cdot}) := T^{-1}(\cdot)$.

Finally, let the state be defined by $x := [\tilde{\imath}_d \ \tilde{\imath}_q \ \tilde{\omega}]^\top$. Then, defining $\widehat{(\cdot)} = \frac{d(\cdot)}{dt}$ the system can be written as:

$$\dot{x}_1 = -x_1 + x_3 x_2 + \hat{u}_d \quad (3a)$$

$$\dot{x}_2 = -x_2 - x_3 x_1 + \gamma x_3 + \hat{u}_q \quad (3b)$$

$$\dot{x}_3 = -\sigma(x_3 - x_2) - \tilde{\tau}_L + \varepsilon x_1 x_2 \quad (3c)$$

The control problem consists now in stabilizing system (3) around an operating regime (x_{1d}, x_{2d}, x_{3d}) moreover, assuming that τ_L is unknown. Furthermore, we shall also consider parametric uncertainty in the other variables.

III. THE CONTROLLER

The control approach consists in exploiting the physical properties of the system. Firstly, we observe that the subsystem given by the first two equations in (3) has a stable equilibrium at the origin whenever $x_3(t)$ is regarded as an external "input", the controls and γ are set to zero; as a matter of fact, the system is input to state stable with respect to the "input" x_3 when $\hat{u}_d = \hat{u}_q \equiv 0$. Hence, the control is designed with aim at:

- keeping the cascaded structure[2];
- choosing an operating point for the current variables x_1 and x_2 such that any desired velocity x_3 can be achieved (different from zero).

To that end, and as the motivation will become clear later, the operating "point" is set to:

$$x_{1d}(t) \neq -\sigma/\varepsilon \quad x_{2d} := x_{3d} + \vartheta + \frac{\dot{x}_{3d}}{\varepsilon x_{1d} + \sigma} \quad (4a)$$

$$\vartheta := \frac{\tilde{\tau}_L - \varepsilon x_{1d} x_{3d}}{\varepsilon x_{1d} + \sigma} \quad (4b)$$

By assumption $\tilde{\tau}_L$ is unknown hence so is the operating point x_{2d}. Introducing an estimate of $\tilde{\tau}_L$ which we denote $\hat{\tau}_L$, we define

$$\text{(set-point)} \quad \hat{x}_{2d} := x_{3d} + \frac{\hat{\tau}_L - \varepsilon x_{1d} x_{3d}}{\varepsilon x_{1d} + \sigma} \quad (5a)$$

$$\text{(tracking)} \quad \hat{x}_{2d} := x_{3d}(t) + \frac{\dot{x}_{3d}(t) + \hat{\tau}_L - \varepsilon x_{1d}(t) x_{3d}(t)}{\varepsilon x_{1d}(t) + \sigma} \quad (5b)$$

and we shall design an adaptation law for $\hat{x}_{2d}$. The control design strategy is, as in [6], to steer $\hat{x}_2$ to x_{2d} and x_2 to $\hat{x}_2$.

Proposition 1 (Set-point control) *Let x_{id}, $i = 1, 2, 3$ be constant. Consider the system (3) in closed-loop with the controller*

$$\hat{u}_d := x_{1d} - \hat{x}_{2d} x_3(t)$$

$$\hat{u}_q := -\gamma x_3(t) + x_{1d} x_3(t) + \hat{x}_{2d}$$

$$\dot{\hat{\tau}}_L := -\alpha' e_3 (\varepsilon x_{1d} + \sigma), \quad \alpha' > 0$$

with $x_{1d} \neq -\sigma/\varepsilon$, $\hat{x}_{2d}$ as in (5a). Define the error variables $e_i := x_i - x_{id}$ and $\bar{x}_{2d} := \hat{x}_{2d} - x_{2d}$. Then, the origin of the closed-loop system i.e. the point $(e_1, e_2, e_3, \bar{x}_{2d}) = (0, 0, 0, 0)$ is globally asymptotically stable.

We shall prove the previous proposition as a corollary of the more general case of trajectory tracking control.

Proposition 2 (Tracking control) *Let $t \mapsto x_{id}$ be continuously differentiable functions, bounded and with bounded derivatives satisfying (4). Consider the system (3) in closed-loop with the controller*

$$\hat{u}_d := x_{1d} - \hat{x}_{2d} x_3(t) + \dot{x}_{1d} \quad (7a)$$

$$\hat{u}_q := -\gamma x_3(t) + x_{1d} x_3(t) + \hat{x}_{2d} + \dot{\hat{x}}_{2d} \quad (7b)$$

$$\dot{\hat{\tau}}_L := -\alpha' e_3 (\varepsilon x_{1d}(t) + \sigma), \quad \alpha' > 0 \quad (7c)$$

[2]We remark at this point that cascades-based design has also been used in [6] for set-point control with known and unknown load torque.

with either $\dot{x}_{1d} \equiv 0$ or $\varepsilon = 0$, $\hat{x}_{2d}$ as in (5b). Define $\bar{x}_{2d} := \hat{x}_{2d} - x_{2d}$. Then, the origin of the closed-loop system i.e. the point $(e_1, e_2, e_3, \bar{x}_{2d}) = (0, 0, 0, 0)$ is uniformly globally exponentially stable.

Proof. *The closed-loop equations.* Define $\hat{e}_2 := x_2 - \hat{x}_{2d}$ hence, we observe the following useful identities: $\hat{e}_2 - e_2 = -\bar{x}_{2d} := x_{2d} - \hat{x}_{2d}$; $e_2 = \hat{e}_2 + \bar{x}_{2d}$ and $x_2 = \hat{e}_2 + \bar{x}_{2d} + x_{2d}$.

Consider first the dynamic equation of the estimation error $\bar{x}_{2d}$. To that end, we differentiate x_{2d} from (4a) to obtain

$$\dot{x}_{2d} := \dot{x}_{3d} + \dot{\vartheta} + \overbrace{\frac{\dot{x}_{3d}}{\varepsilon x_{1d} + \sigma}} \tag{8}$$

$$\dot{\vartheta} = -\frac{(\varepsilon x_{1d} + \sigma)(\varepsilon \dot{x}_{1d} x_{3d} + \varepsilon x_{1d}\dot{x}_{3d}) + (\tilde{\tau}_L - \varepsilon x_{1d} x_{3d})\varepsilon \dot{x}_{1d}}{(\varepsilon x_{1d} + \sigma)^2} \ .$$

Correspondingly, differentiating (5a) we obtain

$$\dot{\hat{x}}_{2d} := \dot{x}_{3d} + \dot{\hat{\vartheta}} + \overbrace{\frac{\dot{x}_{3d}}{\varepsilon x_{1d} + \sigma}} \tag{9}$$

$$\dot{\hat{\vartheta}} = \frac{(\dot{\hat{\tau}}_L - \varepsilon \dot{x}_{1d} x_{3d} - \varepsilon x_{1d}\dot{x}_{3d})}{(\varepsilon x_{1d} + \sigma)} - \frac{(\hat{\tau}_L - \varepsilon x_{1d} x_{3d})\varepsilon \dot{x}_{1d}}{(\varepsilon x_{1d} + \sigma)^2} \ .$$

Define $\alpha(t) := \alpha'(\varepsilon x_{1d}(t) + \sigma)$. Subtracting (8) from (9) and using (7c) we obtain

$$\dot{\bar{x}}_{2d} = -\alpha(t)e_3 + \frac{(\hat{\tau}_L - \tilde{\tau}_L)\varepsilon \dot{x}_{1d}}{(\varepsilon x_{1d} + \sigma)^2} \ . \tag{10}$$

By assumption, either $\dot{x}_{1d} \equiv 0$ or $\varepsilon = 0$. In either case

$$\dot{\bar{x}}_{2d} = -\alpha(t)e_3 \ . \tag{11}$$

Next, we derive the error dynamics for e_1 and $\hat{e}_2$. For this, we use in (3) $\hat{u}_d$ as defined in (7a) and, in (3b), we use $\hat{u}_q = \hat{u}_q \pm \gamma x_3(t)$ and (7b) to obtain

$$\dot{e}_1 = -e_1 + x_3(t)\hat{e}_2 \tag{12a}$$
$$\dot{\hat{e}}_2 = -\hat{e}_2 - x_3(t)e_1 \tag{12b}$$

Finally, the e_3 equation of the error dynamics is obtained by direct computations. Firstly, we add

$$\pm \varepsilon x_{1d} x_2 \pm \varepsilon x_{1d} x_{2d} \pm \sigma(x_{2d} - x_{3d}) = 0$$

to the right-hand-side of Equation (3c) to obtain, using (4),

$$\dot{e}_3 = -\sigma e_3 + (\sigma + \varepsilon x_{1d})e_2 + \varepsilon x_2 e_1 \tag{13}$$

Then, using the identities introduced at the beginning of the proof, in Equation (13) we obtain

$$\dot{e}_3 = -\sigma e_3 + (\sigma + \varepsilon x_{1d})\bar{x}_{2d} + (\sigma + \varepsilon x_{1d})\hat{e}_2 + \varepsilon x_2(t)e_1 \ . \tag{14}$$

Defining $\xi_1 := [e_3 \ \bar{x}_{2d}]^\top$, $\xi_2 := [e_1 \ \hat{e}_2]^\top$ the previous equations can be put together in the compact ("cascaded") form

$$\dot{\xi}_1 = f_1(t, \xi_1) + G(t, \xi_1, \xi_2)\xi_2 \tag{15a}$$
$$\dot{\xi}_2 = f_2(t, \xi_2) \tag{15b}$$

where $G(t, \xi_1, \xi_2) := [g(t, \xi_1, \xi_2)^\top \ [0 \ 0]^\top]^\top$ and

$$f_1(t, \xi_1) := \begin{bmatrix} -\sigma & (\sigma + \varepsilon x_{1d}(t)) \\ -\alpha'(\sigma + \varepsilon x_{1d}(t)) & 0 \end{bmatrix} \xi_1$$

$$g(t, \xi_1, \xi_2) := [\varepsilon(\xi_{22} + \xi_{12} + x_{2d}(t)) \quad (\sigma + \varepsilon x_{1d}(t))]$$

$$f_2(t, \xi_2) := \begin{bmatrix} -1 & \xi_1(t) + x_{3d}(t) \\ -\xi_1(t) - x_{3d}(t) & -1 \end{bmatrix} \begin{bmatrix} \xi_{21} \\ \xi_{22} \end{bmatrix} \ .$$

Forward completeness. Let $[t_\circ, t_{\max})$ denote the maximal interval of definition of solutions and define

$$v_2(\xi_2(t)) := \frac{1}{2}|\xi_2(t)|^2 \ .$$

The total time-derivative of v_2 yields, using (15a),

$$\dot{v}_2(\xi_2(t)) = -|\xi_2(t)|^2 \ .$$

That is,

$$|\xi_2(t)| \le |\xi_2(t_\circ)|\,\mathrm{e}^{-(t-t_\circ)} \qquad \forall\, t \in [t_\circ, t_{\max}) . \tag{16}$$

The interconnection term g in (15a) satisfies, along solutions, and on on the interval of definition of the latter,

$$|g(t, \xi_1(t), \xi_2(t))| \le c + \varepsilon[\,|\xi_{12}(t)| + |\xi_{22}(t)|\,]$$

where c is a positive number independent of the initial conditions –it depends only on bounds on the reference trajectories $x_{2d}(t)$ and $x_{3d}(t)$. Using this, and defining

$$v_1(\xi_1) := \frac{1}{2}|\xi_{11}|^2 + \frac{1}{2\alpha'}|\xi_{12}|^2 \ . \tag{17}$$

it is direct to obtain that the time-derivative of

$$v(t) := v_1(\xi_1(t)) + v_2(\xi_2(t)) , \tag{18}$$

along the trajectories generated by (15a) and (12), satisfies

$$\dot{v}(t) \le c\,|\xi_1(t)|\,|\xi_2(t)| + \varepsilon[\,|\xi_1(t)|^2\,|\xi_2(t)| + |\xi_2(t)|^2\,|\xi_1(t)|\,] \ .$$

Using the triangle inequality on the bound above and (16) we obtain that there exists $c' : \mathbb{R}_{\ge 0} \to \mathbb{R}_{\ge 0}$ such that

$$\dot{v}(t) \le c'(|\xi_2(t_\circ)|)v(t) \qquad \forall\, t \in [t_\circ, t_{\max}) .$$

Integrating on both sides, we obtain that the solutions may not grow to infinity faster than exponentially and that $t_{\max}$ isfinite.

Stability. Since the system is forward complete, we can view it as a cascaded nonlinear time-varying system –*cf.*[24]. Then, the stability analysis is considerably simplified.

Firstly we observe that the system $\dot{\xi}_2 = f_2(t, \xi_2)$ has a globally exponentially stable equilibrium at the origin. A simple inspection shows the same property for system $\dot{\xi}_1 = f_1(t, \xi_1)$. By assumption, either $\varepsilon = 0$ or x_{1d} is constant hence, $\dot{\xi}_1 = f_1(t, \xi_1)$ is linear time-invariant; its characteristic polynomial is either

$$\lambda^2 + \lambda\sigma + (\varepsilon x_{1d} + \sigma)^2 \alpha' = 0$$

for $\varepsilon \ne 0$ and constant $x_{1d} > -\sigma/\varepsilon$ or,

$$\lambda^2 + \lambda\sigma + \sigma^2 \alpha' = 0$$

for $\varepsilon = 0$ and possibly time-varying x_{1d}. In either case, the origin is exponentially stable for any $\alpha' > 0$.

Uniform global exponential stability of $(\xi_1, \xi_2) = (0, 0)$ follows observing that g in (15a) has linear growth with respect to ξ_1 and invoking a theorem along the lines of the main result in [25], more precisely we can invoke [26, Theorem 4]. Finally, we observe that

$$\begin{bmatrix} \bar{x}_{2d} \\ e_2 \end{bmatrix} = \begin{bmatrix} 1 & 0 \\ 1 & 1 \end{bmatrix} \begin{bmatrix} \bar{x}_{2d} \\ \hat{e}_2 \end{bmatrix} \ .$$

The result follows. ∎

IV. ISS OF THE CLOSED-LOOP SYSTEM

Even though the model (1) covers a number of case-studies used in the literature important physical aspects which entail current-dependence variations of inductances are neglected. The errors caused by neglecting these phenomena which affect the machine performance under specific regimes may be, to some extent, compensated for by introducing parametric uncertainty and additive disturbances to the model (1). We show that the controllers of Proposition 2 render the closed-loop system ISS with respect to external perturbations. In addition, in the following section we illustrate in simulation the robustness of our controllers with respect to measurement noise.

$$\hat{u}_d(x_3) \quad := \quad \hat{u}_d(x_3)^* + \nu_1 \tag{19a}$$

$$\hat{u}_q(x_3) \quad := \quad \hat{u}_q(x_3)^* + \nu_2 \tag{19b}$$

where ν_1 and ν_2 are considered to be external (additional) inputs; these may contain perturbations to the system, measurement noise, additional control terms, *etc.* The closed-loop equations with (3a) and (3b) yield

$$\dot{e}_1 \quad = \quad -e_1 + x_3(t)\hat{e}_2 + \nu_1 \tag{20a}$$

$$\dot{\hat{e}}_2 \quad = \quad -\hat{e}_2 - x_3(t)e_1 + \nu_2. \tag{20b}$$

Define $V(\xi_2) := 0.5\xi_2^2$ with $\xi_2 = \mathrm{col}[e_1\,\hat{e}_2]$ and $\nu = \mathrm{col}[\nu_1\,\nu_2]$. The time derivative of $V(\xi_2)$ along the trajectories of (20) yields

$$\dot{V}(\xi_2) \leq -|\xi_2|^2 + \xi_2^\top \nu \tag{21}$$

From (21) one can see that the system is ISS from the input ν with state ξ_2. Indeed, let $|\nu|_{[t_\circ, t)}$ denote the $\sup\limits_{\tau \in [t_\circ, t)} |\nu(\tau)|$; using this and integrating along trajectories we obtain

$$|\xi_2(t)| \leq |\xi_2(t_\circ)|\, \mathrm{e}^{-\frac{1}{2}(t-t_\circ)} + \frac{1}{2}\,|\nu|_{[t_\circ, t)}. \tag{22}$$

Thus, roughly speaking, the tracking errors ξ_2 converge to a neighborhood of the origin, proportional to the size of the perturbation. A natural requirement is to reduce the size of this neighborhood that is, to impose an error tolerance despite the perturbations. This is a *direct* modification that can be carried out to the controller (7) provided that we add current feedback. Indeed, let ν_1 and ν_2 in (19) be defined by

$$\nu_1 \quad := \quad -k_1 e_1 + d_1(t) \tag{23a}$$

$$\nu_2 \quad := \quad -k_2 e_2 + d_2(t) \tag{23b}$$

where $k_i \geq 0$ are design parameters and d_i now play the role of disturbances. Restarting the above computations from (21) we obtain, defining $k_m := \min\{k_1, k_2\}$ and $d = (d_1\, d_2)^\top$,

$$\dot{V}(\xi_2) \leq -(k_m + 1)\,|\xi_2|^2 + \xi_2^\top d.$$

Hence,

$$|\xi_2(t)| \leq |\xi_2(t_\circ)|\, \mathrm{e}^{-\frac{k_m+1}{2}(t-t_\circ)} + \frac{1}{2(k_m+1)}\,|d|_{[t_\circ, t)} \tag{24}$$

It is clear that for $k_i = k_m = 0$ that is, if no current feedback is applied, we recover the inherent robustness expressed by (22) however, for positive values of k_m we see that the currents errors converge to the interior of a ball that depends on the norm of d but may be diminished at will, by enlarging k_m.

More "sophisticated" controls may be used: the gains k_1, k_2 may be functions of the state as opposed to constants. For instance, we may decide to make k_i depend on the currents values *i.e.*, $k_i := k_i(e_i)$. Let us reconsider (21) with ν as in (23) and k_i as defined above. We see that

$$\dot{V}(\xi_2) \leq -\sum_{i=1}^{2}[e_i^2[1 + k_i(e_i)] - e_i d_i].$$

Then, the requirement is that the functions k_i be such that:

(i) $k_i(e_i) \geq 0 \quad \forall\, e_i \in \mathbb{R}$;

(ii) for ISS to hold, there must exist class $\mathcal{K}$ function μ such that

$$\text{whenever} \quad \frac{[k_i(e_i) + 1]e_i^2}{|e_i|} \geq |d_i| \quad \text{with } i \in \{1, 2\}$$

$$\text{we have} \quad \dot{V}(\xi_2) \leq -\mu(|\xi_2|).$$

Other "sector" nonlinearities may be of interest. For instance, one may use saturation terms such as $-k_i\mathrm{sat}(e_i)$ with $\mathrm{sat}(\cdot)$ being a smooth saturation function, such as $\tanh(\cdot)$ or smooth "dead-zone" curves such as $a\tanh(b\sinh(cx))|x|$. For suitably chosen parameters a, b and c this curve may be designed to be "approximately" linear with unitary slope outside of a neighborhood of $x = 0$ and have a very small slope inside the neighborhood. One use of such function may be to avoid large overshoots. The functions k_i may also be chosen to depend on the *velocity* errors e_3. For instance, it seems reasonable that, since the variable of main interest is e_3 we make the control gains large only for "large" velocity errors hence, we define $k_i := k_i(|e_3|)$ with k_i of class $\mathcal{K}$. The proofs for all these cases remain *unchanged*. Moreover, it should be clear that the calculations and discussion above hold for all cases previously studied: set-point and tracking with known and with unknown load.

V. SIMULATIONS

We have used SIMULINK™ of MATLAB™ to test our controllers in numeric simulations. The benchmark model is taken from the literature –*cf.* [5] and is as follows: we set the system parameters to values leading to chaotic behavior in open loop *i.e.*, $\sigma = 5.46$, $\gamma = 30$, $\varepsilon = 0$ $\tilde{\tau}_L = 10$ and initial state values of 0.01. Several sets of simulations are presented covering the cases with and without disturbances and with and without load estimation. These simulation results illustrate the performance and robustness of all controllers previously introduced.

We use the adaptive controller of Proposition 2 under different conditions: with and without current feedback and with and without (time-varying) parametric uncertainty, additive disturbances and measurement noise. When we use the current feedback terms –*cf.* Eq. (23) both gains are set to $k_1 = k_2 = k = 20$. The adaptation gain in (7c) is set to $\alpha = 3$ and $\alpha = 30$. Measurement noise, disturbances and time-varying parametric uncertainty are generated by random normal Gaussian signals; parametric uncertainty varies from 0 to 20%. In the simulation experiment controls are switched on at $t = 15s$, the normalized reference signal $x_{3d}(t)$ changes from different regimes going from sinusoidal (period $= 2\pi$ and amplitude equal to 100) to steps (150 and zero) and finally to a chaotic regime. Reference
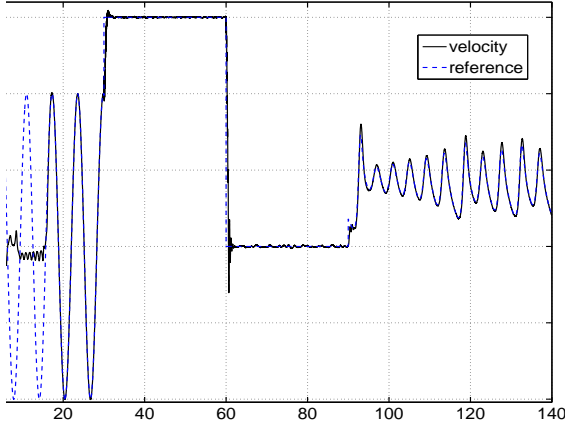
Fig. 1. Graph of the normalized velocity and reference in the worst-case scenario: without $k = 0$ in (23), uncertainty and noise.

changes occur at $t = 30s$, $t = 60s$ and $t = 90s$. The simulation results are showed in Figures 1-5.

In Figure 1 we show the system's normalized-velocity response in the worst-case scenario: no current feedback — $k = 0$ in (23), presence of additive disturbances, parametric uncertainty and measurement noise. The figure shows both the system's actual trajectory $x_3(t)$ and its reference $x_{3d}(t)$. For the sake of
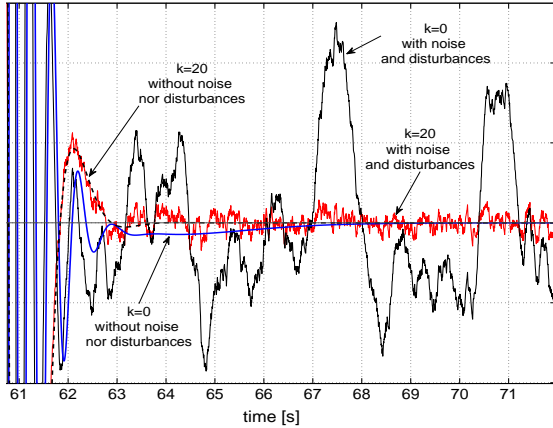

Fig. 2. Zoom on the normalized velocity transient for the second step and reference in four scenarios.

comparison in Figure 2 we show a zoom on the system's response (normalized velocity $x_3(t)$) in the four different scenarios. The window shows the transient response from the first step (to 150) to a steady-state zero-velocity reference, over the first 10 seconds. One can appreciate that, in the absence of noise and disturbances, the transient duration is significantly reduced using the state feedback terms in (23). Correspondingly in the case of parametric uncertainties and noise, the effect of the latter is significantly reduced via the controls from Section IV. In Figure 3 we show the normalized velocity errors $e_3(t)$ for three different cases with and without noise and disturbances and with ($k = 20$) and without ($k = 0$) current feedback. From the zoomed plots
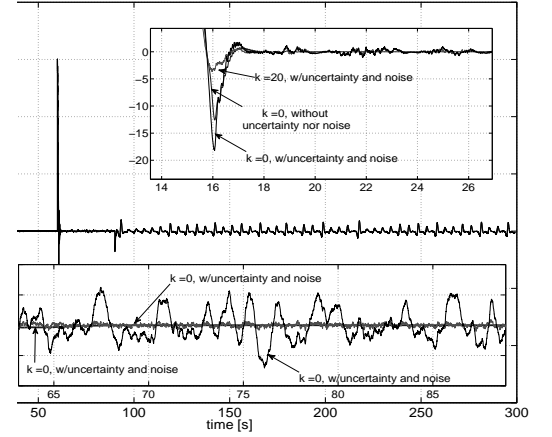

Fig. 3. Graph of the normalized velocity errors and zooms. Three cases showed: (1) without extra gain ("$k = 0$") and without uncertainty nor noise; (2) with $k = 0$, uncertainty and noise and with extra gain $k = 20$ (current feedback), uncertainty and noise.

one can clearly appreciate both the transient and steady-state improvement when additional feedback is used, as discussed in Section IV. Also, observe in the lower zoomed window in the zero-error in the ideal case when there is no parametric uncertainty nor noise even when no extra current feedback is used; that is using the output-feedback adaptive algorithm from Proposition 2. Finally, we remark from Figure 3 the steady-state oscillatory behavior of the velocity error when tracking the Lorenz reference (for $t \geq 90s$); as we show in Figure 4, this error may be attenuated by increasing the adaptive gain α in (7c). Similar performance is observed for the estimation error $\hat{e}_2(t)$ in Figure 5.
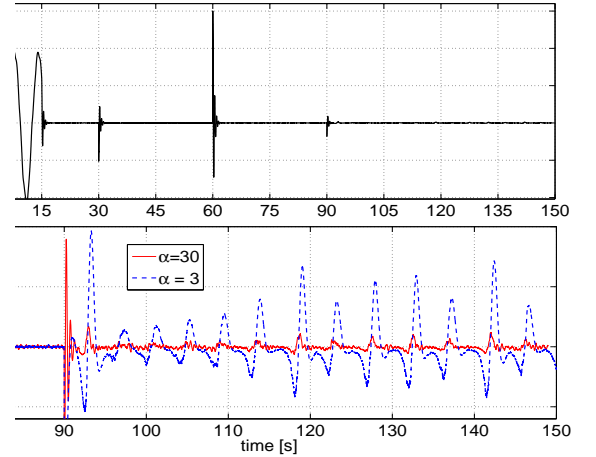

Fig. 4. Zoom on the normalized velocity errors during transient under state-feedback control. Two cases showed: $\alpha = 30$ and $\alpha = 3$; additive disturbances, measurement noise and time-varying parametric uncertainty present in both cases.

Remark 1 Regarding the Gaussian parametric variation considered in the simulation it goes without saying that an electronic component is not meant to vary *randomly* however, variations may be due to different phenomena, caused by many external
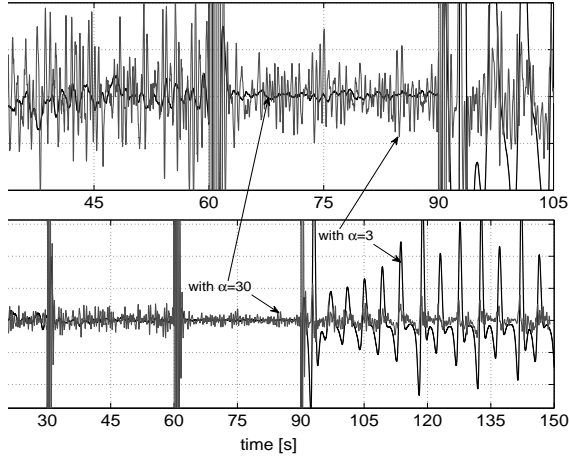
Fig. 5. Estimation errors $\hat{e}_2(t)$ during transient, under state-feedback control, additive disturbances, measurement noise and time-varying parametric uncertainty. Two cases showed: $\alpha = 30$ and $\alpha = 3$.

unpredictable 'agents' affecting the system such as temperature which affects resistance not mentioning the simplistic model used which disregards nonlinear dependence of inductance with respect to angular position and current. Now, if we consider the case of inductances depending *only* on rotor position and we consider that the rotor position is to undergo a chaotic regime as much as constant or a sinusoidal the graph of the inductance variation *as function of time* may have an infinite number of "shapes". In this regard, it does not seem unnatural that a wide variety of possibilities regarding the variations of parametric uncertainty, around an average constant value may be covered by *randomly*-generated signals. Thus, in the simulation we consider $\sigma(t_k) = \sigma_o + v(t_k)$ where σ_o is a nominal value and $v(t_k)$ is a number randomly generated at each integration step t_k.

VI. CONCLUSION

We have showed that adaptive tracking output regulation of PMSMs is achievable via a simple linear output feedback controller, provided that one chooses adequately the operating point for the quadrature axis current. Uniform global exponentially stable hence, ISS is proved. Robustness to measurement noise and parametric uncertainty is illustrated by simulations.

REFERENCES

[1] Z. Li, B. Zhang, and Z. Mao, "Analysis of the chaotic phenomena in permanent-magnet synchronous motors based on Poincaré map," in *3rd World Congress on Intelligent Control and Automation*, (Hefei, China), pp. 3255–3260, 2000.

[2] N. Hemati and H. Kwati, "Bifurcation of equilibria and chaos in permanent-magnet machines," in *Proc. 32nd. IEEE Conf. Decision Contr.*, (San Antonio, TX, USA), pp. 475–480, 1993.

[3] X. Ge and J. Huang, "Chaos control of permanent-magnet synchronous motor," in *International Conference on Electrical Machines and Systems*, vol. 1, pp. 484–488, 2005.

[4] N. Hemati, "Strange attractors in brushless DC motors," *IEEE Trans. on Circ. Syst. I: Fundamental Theory and Applications*, vol. 41, no. 1, pp. 40–45, 1994.

[5] H. Ren and D. Liu, "Nonlinear feedback control of chaos in permanent-magnet synchronous motor," *IEEE Trans. on Circ. Syst. II: Express Briefs*, vol. 53, no. 1, pp. 45–50, 2006.

[6] V. Petrović, R. Ortega, and A. M. Stanković, "Interconnection and damping assignement approach of PM synchronous motors," *IEEE Trans. Contr. Syst. Technol.*, vol. 9, no. 6, pp. 811–821, 2001.

[7] H. Yu, H. Wang, and K. Zhao, "Energy-shaping of PM synchronous motor based on Hamiltonian systems theory," in *International Conference on Electrical Machines and Systems*, vol. 2, pp. 1549–1553, 2005.

[8] D. Q. Wei, X. S. Luo, B. H. Wang, and J. Q. Fang, "Robust adaptive dynamic surface control of chaos in permanent magnet synchronous motor," *Phys. Lett. A*, vol. 363, no. 1–2, p. 71, 2007.

[9] Z. Wang and K. T. Chau, "Anti-control of a permanent-magnet DC motor system for vibratory compactors," *Chaos Solitons and Fractals*, vol. 36, pp. 694–708, 2008.

[10] H. P. Ren and C. Z. Han, "Chaotifying control of permanent-magnet synchronous motor," in *Power Electronics and Motion Control Conf.*, vol. 1, pp. 1–5, 2006.

[11] C. J. Retter, *Matrix and space-phasor theory of electrical machines*. Budapest: Akadémiai Kiadó, 1987.

[12] Z. Li, J. B. Park, Y. H. Joo, B. Zhang, and G. Chen, "Bifurcations and chaos in a permanent-magnet synchronous motor," *IEEE Trans. on Circ. Syst. I: Fundamental Theory and Applications*, vol. 49, no. 3, pp. 383–387, 2002.

[13] C. Cai, Z. Xu, and W. Xu, "Converting chaos into periodic motion by state-feedback control," *Automatica*, vol. 38, pp. 1927–1933, 2002.

[14] D. Liu, H. Ren, and X. Liu, "Chaos control in permanent-magnet synchronous motor," in *International Sympsium on Circuits and Systems*, vol. 4, pp. 732–735, 2004.

[15] V. Petrović, R. Ortega, A. M. Stanković, and G. Tadmor, "Design and implementation of an adaptive controller for torque ripple minimization in PM synchronous motors," *IEEE Transactions on Power Electronics*, vol. 15, no. 5, pp. 871–880, 2000.

[16] F. Poulin, L. Praly, and R. Ortega, "An observer for permanent magnet synchronous motors with application to sensorless control," in *Proc. 47th. IEEE Conf. Decision Contr.*, (Cancún, México), p. to appear, 2008.

[17] Y. Yan, J. Zhu, H. Lu, Y. Guo, and S. Wang, "A PMSM model incorporating structural and saturation saliencies," in 8th *Internation Conference on Electrical Machines and Systems*, vol. 1, pp. 194–199, 27-29 sept. 2005.

[18] Y. Yan, J. Zhu, Y. Guo, and H. Lu, "Modeling and simulation of direct torque controlled PMSM drive system incorporat structural and saturation saliencies," in *41st Industry Applications Conference*, vol. 1, pp. 76–83, 27-29 oct. 2006.

[19] Y. Yan, J. Zhu, H. Lu, Y. Guo, and S. Wang, "A direct torque controlled surface mounted PMSM drive with initial rotor position estimation based on structural and saturation saliencies," in *42nd Industry Applications Conference*, vol. 1, pp. 683–689, 23-27 sept. 2007.

[20] Y. Ying, Z. Jianguo, G. Youguang, and J. Jianxun, "Numerical simulation of a PMSM model considering saturation saliency for initial rotor position," in 27th *Chinese Control Conference*, (Kunming, China), pp. 114–118, July 16–18 2008.

[21] M. Hadžiselimović, G. Štumberger, B. Štumberger, and I. Zagradišnik, "Magnetically nonlinear dynamic model of synchronous motor with permanent magnets," *Journal of Magnets and Magnetic Materials*, no. 317, pp. 257–260, 2007.

[22] N. Goléa, A. Goléa, and M. Kadjoudj, "Robust MRAC adaptive control of PMSM drive under general parameters uncertainties," in *IEEE Int. Conf. on Industrial technology*, pp. 1533–1537, 2006.

[23] J. Kabziński, "Adaptive backstepping control of a completely unknown permanent magnet motor," in *European Conference on Power Electronics and Applications*, pp. 1–10, 2–5 sept 2007.

[24] A. Loría, "From feedback to cascade-interconnected systems: Breaking the loop," in *Proc. 47th. IEEE Conf. Decision Contr.*, (Cancun, Mex.), pp. 4109–4114, 2008.

[25] A. Saberi, P. V. Kokotović, and H. J. Sussmann, "Global stabilization of partially linear systems," *SIAM J. Contr. and Optimization*, vol. 28, pp. 1491–1503, 1990.

[26] E. Panteley and A. Loría, "Growth rate conditions for stability of cascaded time-varying systems," *Automatica*, vol. 37, no. 3, pp. 453–460, 2001.